Friction-Based Design of Kinematic Couplings

Layton C. Hale
Lawrence Livermore National Laboratory
Livermore, CA 94550

Abstract

Friction affects several aspects important to the design of kinematic couplings, but particularly the ability to reach its centered position is fundamental.[1] It becomes centered when all pairs of contacting surfaces are fully seated even though a small uncertainty may exist about the exact center where potential energy is minimum. For many applications, centering ability is a good indicator for optimizing the coupling design. Typically, the coupling design process has been largely heuristic based on a few guidelines [Slocum, 1992]. Several simple kinematic couplings (for example, a symmetric three-vee coupling) are compared for centering ability using closed-form equations. More general configurations lacking obvious symmetries are difficult to model in this way. A unique kinematic coupling for large interchangeable optics assemblies in the National Ignition Facility motivated the development of a computer program to optimize centering ability. However, space limits the description of the program to the basic algorithm. Currently the program is written in Mathcad™ Plus 6 and is available upon request.[2]

Background

Kinematic couplings serve many applications that require: 1) separation and repeatable engagement, and/or 2) minimum influence that an imprecise or unstable foundation has on the stability of a precision component. An object that is rigid, relatively speaking, requires six independent constraints to exactly constrain six rigid-body degrees of freedom. An object with one or more flexural degrees of freedom requires additional constraints; for example, a four-legged chair flexes torsionally to fit the shape of the floor. This paper deals only with six-constraint couplings supported through local surfaces and held in contact by a consistent nesting force. Quite often the nesting force is the weight of the object being supported, or it may result from a spring or other force device. Ideally, the nesting force causes all surfaces to engage freely and with uniform loading.

Figure 1 shows the two classic types of kinematic couplings, the three-vee coupling (left) and the cone-vee-flat coupling (right). The symmetry of three vees offers several advantages: more uniform contact stresses, thermal expansion about a central point and reduced manufacturing costs due to identical features. Conversely, the cone (or the more kinematically correct tetrahedral socket) offers a natural pivot point for angular adjustments. The three-vee coupling is the natural choice for adjustments in six degrees of freedom.

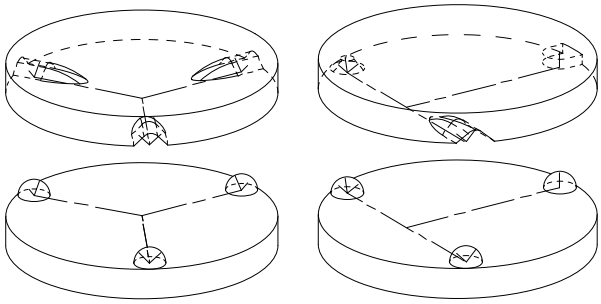

Figure 1 The three-vee coupling has six constraints arranged in three pairs. The cone-vee-and-flat coupling has six constraints arranged in a 3-2-1 configuration.

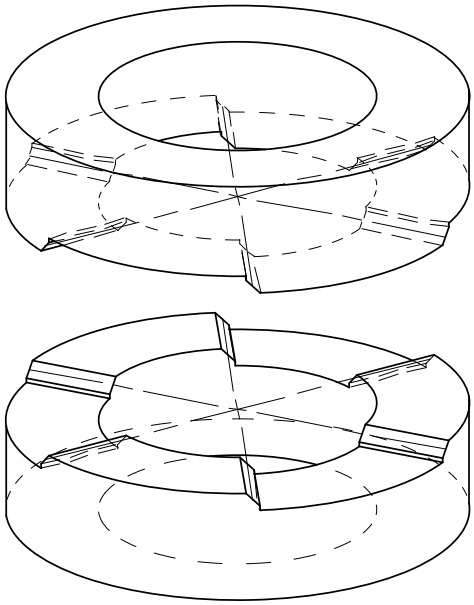

Figure 2 The three-tooth coupling forms three theoretical line contacts between cylindrical teeth on one half and flat teeth on the other half.

This work was performed under the auspices of the U.S. Department of Energy by Lawrence Livermore National Laboratory under contract No. W-7405-Eng-48.

[1] In this paper, the term kinematic coupling refers to any connection device based on pairs of contacting surfaces that provide six constraints in an ideal sense.

[2] Email requests to hale6@llnl.gov.

The local contact areas typical of these kinematic couplings are quite small and require a Hertzian analysis to ensure a robust design. Greater durability is achieved by curvature matching such as a ball against a concave surface and/or by using ceramic materials such as silicon nitride balls against tungsten carbide gothic arches. Designs based on line contact rather than point contact offer a significant increase in load capability. For example, a kinematic equivalent to three vees is a set of three balls in three conical sockets with either the balls or the sockets supported on radial-motion flexures. Alternatively, the three-tooth coupling shown in Figure 2 is based on three theoretical lines of contact formed between cylindrical and flat teeth. Each line constrains two degrees of freedom giving a total of six constraints. Manufactured with three identical cuts directly into each coupling half, the teeth must be straight along the lines of contact but other tolerances can be relatively loose.

Friction Effects

Friction affects at least four important characteristics of a kinematic coupling as indicated by order-of-magnitude estimates that all include the coefficient of friction μ.

1) Repeatability $$\frac{f}{k} \approx \mu \left(\frac{2}{3R} \right)^{1/3} \left(\frac{P}{E} \right)^{2/3}$$

2) Kinematic support $$|f_t| \le \mu \, f_n$$

3) Stiffness $$k_t = k_n \frac{2 - 2\nu}{2 - \nu} \left(1 - \frac{f_t}{\mu \, f_n} \right)^{1/3} \approx 0.83 k_n$$

4) Centering ability $$\frac{f_c}{f_n} \approx 0.5 - 1.3\mu$$

Tangential friction forces at the contacting surfaces may vary in direction and magnitude depending how the coupling comes into engagement. This affects the repeatability of the coupling and the kinematic support of the precision component. The estimate for repeatability is the unreleased frictional force multiplied by the coupling's compliance. The estimate is derived as if the coupling's compliance in all directions is equal to a single Hertzian contact carrying a load P and having a relative radius R and elastic modulus E. The frictional force acts to hold the coupling off center in proportion to the compliance. This estimate will underestimate the repeatability if the structure of the coupling is relatively compliant compared to the contacting surfaces.

Kinematic support is important for stability of shape of the precision component. The estimate for kinematic support simply gives a bound on the magnitude of friction force acting at any contact surface. A sensitivity analysis of the precision component will determine a tolerable level of friction that the coupling can have. This may drive the design to include flexure elements and/or procedures to release stored energy. If repeatable engagement is not so important, then constraints using rolling-element bearings offer very low friction. For example, a pair of cam followers that contact with crossed axes is equivalent to a ball on a flat but with twenty or so times less friction.

In some cases frictional overconstraint is valuable for increasing the overall system stiffness. Provided the tangential force is well below what would initiate sliding, the tangential stiffness of a Hertz contact is comparable to the normal stiffness [Johnson, 1985]. This was important for the National Ignition Facility where frictional overconstraint stiffened the first torsional mode of optics assemblies sufficiently to meet dynamic stability requirements.

Centering ability can be expressed as the ratio of centering force to nesting force and the estimate shown is typical. A larger ratio means the coupling is better at centering in the presents of friction. Later, it is convenient to express centering ability as the coefficient of friction where the ratio goes to zero. For the estimate, the limiting coefficient of friction is 0.5/1.3 = 0.38. The coupling will center if the real coefficient of friction is less than the limiting value.

Centering Ability

The contacting surfaces of a kinematic coupling come into engagement sequentially unless it is placed precisely at the exact center. The path to center is constrained by the surfaces already in contact. For example, five surfaces in contact constrain the coupling to slide along a well-defined path. Four surfaces in contact allow motion over a two-dimensional surface of paths and so forth. Although there are infinitely many paths to center, only the limiting case is of practical interest for determining centering ability. Further, it is reasonable to expect the limiting case to be one of six possible paths that have five surfaces in contact.[3] This point is demonstrated using the three-vee coupling.

For any given path to center, the centering force that results from the nesting force may be derived using Statics and the Coulomb law of friction. Figure 3 shows

[3] The exception to this statement is the ball-cone constraint of the cone-vee-flat coupling since the cone provides only one constraint until the ball is fully seated. A tetrahedral socket remedies this situation.

examples of centering force (per unit nesting force) plotted versus the coefficient of friction. These curves were generated from closed-form equations yet to be discussed. Although the curves look simple, the equations are rather tedious to develop even when the coupling has simple geometry and the load is symmetrical. Compound this with the possible number of paths to center and it becomes obvious that a systematic, computer-based approach is essential for designing more general configurations of couplings.

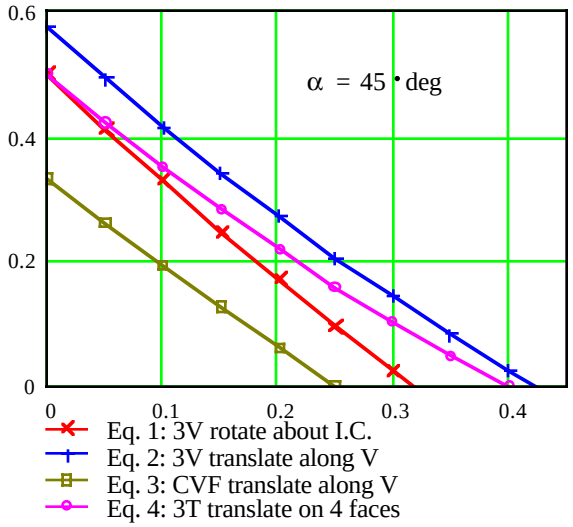

Figure 3 Centering force versus coefficient of friction.

Figure 4 shows a symmetric three-vee coupling rotating about its instant center to reach the center position. This path has five surfaces in contact and is the limiting case along with five other symmetrically identical paths. Equation 1 provides the centering force for this path assuming the nesting force is uniformly carried by three balls. Note, the sides of the vees are an angle α with respect to the plane of the three balls. In addition, there are two sets of symmetrically identical paths having four surfaces in contact. Equation 2 provides the centering force for the more limiting path where the coupling translates radially along one vee. The other path is rotation about one ball.

$$\frac{f_c}{f_n} = \frac{\sin\alpha - \mu\cos\alpha}{2(\cos\alpha + \mu\sin\alpha)} - \frac{\sqrt{3}\,\mu}{3\cos\alpha} \qquad (1)$$

$$\frac{f_c}{f_n} = \frac{\sqrt{3}\,\sqrt{4+3\tan^2\alpha}\,\sin\alpha - 4\mu}{3\left[\sqrt{4+3\tan^2\alpha}\,\cos\alpha + \sqrt{3}\,\mu\tan\alpha\right]} - \frac{\mu}{3\cos\alpha} \qquad (2)$$

This example shows that the path with five surfaces in contact has less centering force than either path with four surfaces in contact. This may not be universally true for a general kinematic coupling. That is, a path with five surfaces in contact may have greater centering force than another path with four surfaces in contact. However as the coupling continues toward center, the centering force cannot increase as it picks up the fifth contact surface. Thus, we need only look at paths with five surfaces in contact to determine the limiting case.

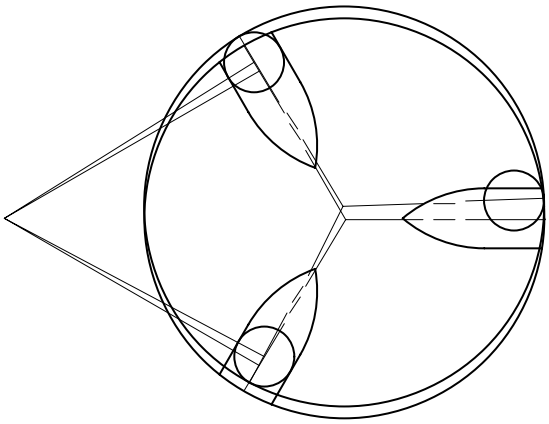

Figure 4 The limiting case for centering occurs when the three-vee coupling slides on five surfaces producing rotation about its instant center.

It is also useful to compare the centering forces for the other types of kinematic couplings. Figure 5 shows the cone-vee-flat coupling translating along its vee. This path is underdetermined for a conical socket but is representative of the limiting case. It was chosen to simplify the expression for centering force given in Equation 3. Referring back to Figure 3, it may come as a surprise that the cone-vee-flat coupling has the least centering ability of the three types. However, significant improvement is possible by carrying more load with the cone and by increasing the cone angle.

$$\frac{f_c}{f_n} = \frac{\sin\alpha - \mu\cos\alpha}{3(\cos\alpha + \mu\sin\alpha)} - \frac{\mu}{3\cos\alpha} - \frac{\mu}{3} \qquad (3)$$

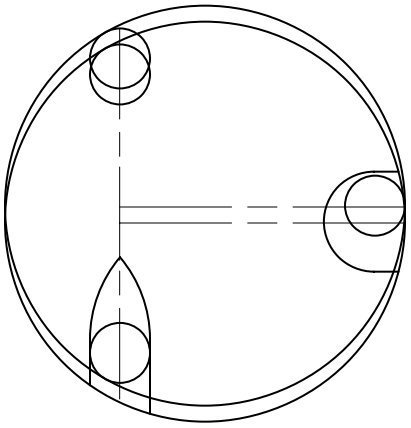

Figure 5 The limiting case for centering occurs when the cone-vee-flat coupling slides on the vee and flat with the cone seeking center.

Equation 4 gives the centering force for the three-tooth coupling as it translates on four surfaces. The centering force with five surfaces in contact is very difficult to model in closed form but behaves similarly to the limiting case for the three-vee coupling. For example, the limiting coefficient of friction for the three-tooth coupling is 0.319 at $\alpha = 45^\circ$ or 0.352 at $\alpha = 60^\circ$. The limiting coefficient of friction for the three-vee coupling is 0.317 at $\alpha = 45^\circ$ or 0.364 at $\alpha = 60^\circ$.

$$\frac{f_c}{f_n} = \frac{\sqrt{4+\tan^2\alpha}\,\sin\alpha - 4\mu}{2\left[\sqrt{4+\tan^2\alpha}\,\cos\alpha + \mu\tan\alpha\right]} \qquad (4)$$

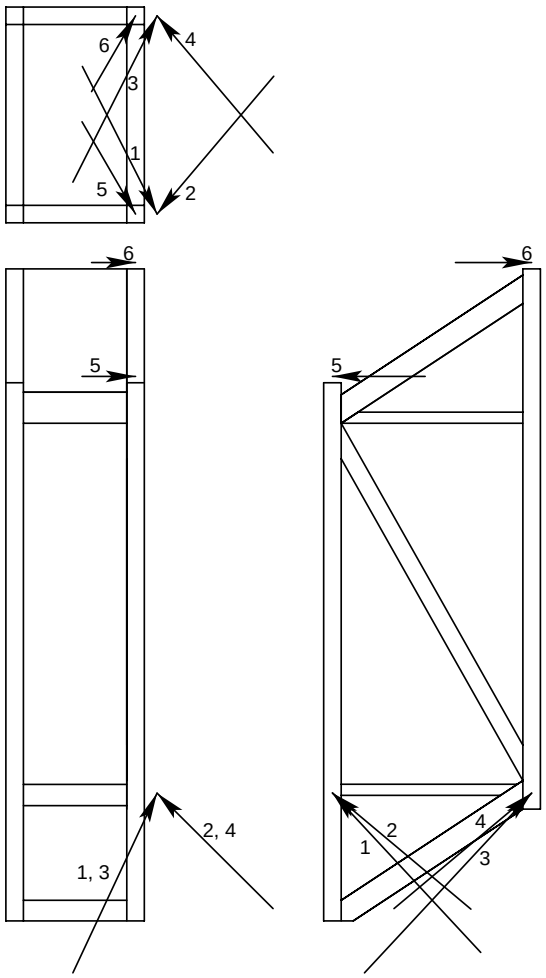

Figure 6 Three views of the optic assembly supported by six constraints. The arrows are proportional to forces.

Centering Optimization Algorithm

As discussed, the limiting coefficient of friction occurs along a path defined by five surfaces in contact. There are six such paths each corresponding to one of six surfaces not in contact. Using [6 x 6] transformation matrices, it is straight forward to reflect contact stiffnesses to a global coordinate system (CS). Adding any five results in a stiffness matrix for the coupling that has zero stiffness along the path. The eigenvector corresponding to the zero eigenvalue gives the direction that the coupling slides in the global CS. Using the same transformation matrices, a local sliding vector is determined for each surface. Then a force-moment vector is calculated for each surface using the Coulomb law of friction and a unit normal force. Transforming back to the global CS, the vectors are assembled into a matrix that when multiplied by a vector of contact forces gives the force-moment resultant on the coupling. The inverse of the matrix is useful because it gives the contact forces for a given coefficient of friction and applied load. Then the equation for the surface not in contact is solved for the coefficient of friction that makes its normal force zero. This is done for each surface not in contact, and the minimum is the limiting coefficient of friction.

Figure 6 shows one example of an optics assembly for the National Ignition Facility. This example has four angular parameters: the axis angle of two vee blocks (constraints 1-2 and 3-4); the more shallow face angle of the vee blocks (constraints 1-3); the steeper face angle (constraints 2-4); and the angle of the upper constraints. The user determines the optimum by adjusting the nominal parameter vector θ based on curves that show the effect of individually varying parameters. Figure 7 shows the optimal parameter set for this example.

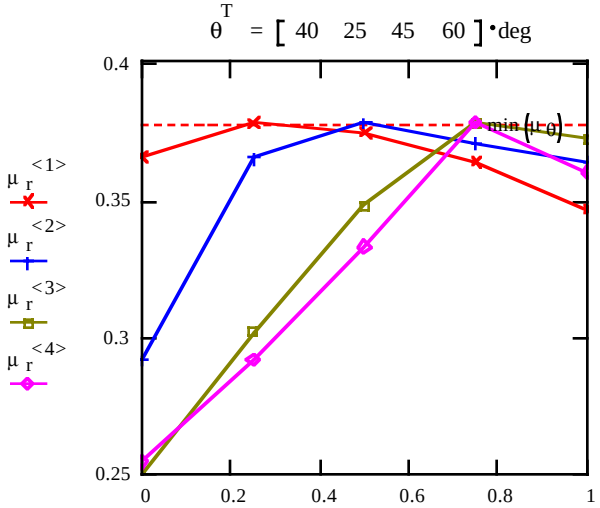

Figure 7 Limiting coefficient of friction versus varying model parameters. All curves pass through the nominal parameter set as indicated by the dashed line.

References

Johnson, K. L. "Contact Mechanics" Cambridge University Press, 1985

Slocum, Alexander H. "Precision Machine Design" Prentice Hall, Englewood Cliffs, New Jersey, 1992